Heart Failure Clinic,
ISSN / eISSN 1551-7136
Publisher ELSEVIER SCIENCE INC,
STE 800, 230 PARK AVE,NEW YORK,
USA, NY, 10169
Volume 26-Issue 1-(2026)
DOI:https://doi.org/10.65281/738001

Prediction of Orthodontic Force Generated By Intrusion Arch Using Multiple Regression Analysis and Artificial Neural Networks

Jingchao Wang[1], Wenbo Ji[2], Liang Yao[3], Zhixian Qiu[4], Dianhao Wu[5], Hanlin Wang[6], Shan Zhou[7], Xiaofeng Wang[8]

[1] The Second Affiliated Hospital of Harbin Medical University, Harbin, Heilongjiang, China
[2] The Second Affiliated Hospital of Harbin Medical University, Harbin, Heilongjiang, China
[3] Linyi University, Linyi, Shandong, China
[4] Harbin University of Science and Technology, Harbin, Heilongjiang, China
[5] University of Science and Technology Liaoning, Anshan, Liaoning, China
[6] Jinzhou Medical University, Jinzhou, Liaoning, China
[7] The Second Affiliated Hospital of Harbin Medical University, Harbin, Heilongjiang, China
[8] Harbin Medical University, Harbin, Heilongjiang, China

Corresponding authors:
Shan Zhou (h04380@hrbmu.edu.cn)
Xiaofeng Wang (13633617656@163.com)

KEYWORDS: Intrusion arch; prediction of orthodontic force; artificial neural networks; multivariate regression analysis; correlation analysis

SUMMARY:

This protocol aims to develop and validate predictive models for orthodontic force generated by an intrusion arch using multiple nonlinear regression analysis (MNLA) and artificial neural networks. The MNLA model demonstrated superior accuracy, with a clinically applicable mean absolute percentage error of 3.66%, identifying arch height as the most influential parameter.

ABSTRACT:

This study aims to develop predictive models for orthodontic force using multiple regression analysis (MRA) and artificial neural networks (ANNs), enabling parametric representation and accurate prediction of applied force. A total of 300 samples were collected to measure the characteristic parameters of intrusion arches—arch length, height, and bending angle—and their corresponding orthodontic force. A comprehensive database was constructed to analyze the correlation between each parameter and the force. Four predictive models were established using MRA and ANN methodologies. Their accuracy was evaluated using root mean squared error (RMSE), mean absolute error (MAE), mean absolute percentage error (MAPE), and coefficient of determination (R^2). A statistically significant correlation ($p < 0.001$) was found between orthodontic force and the three parameters, with influence ranked as: arch height > bending angle > arch length. Comparative analysis revealed that the multiple nonlinear regression analysis (MNLA) model demonstrated the best predictive performance, achieving superior fitting and the lowest prediction error in both the training and testing datasets, with R^2 values of 0.934 and 0.900, RMSE values of 1.050 and 0.988, MAE values of 0.834 and 0.772, and MAPE values of 4.09% and 3.66%, respectively. The ANN model using Rectified Linear Unit activation also showed strong performance, with a slightly higher testing set MAPE of 4.17%, indicating its potential applicability where nonlinear modeling is preferred. These findings suggest that the orthodontic force generated by an intrusion arch can be effectively modulated by adjusting its characteristic parameters and that the MNLA model provides clinicians with a precise and efficient method for predicting orthodontic force in clinical practice.

INTRODUCTION:

Malocclusion is a common oral condition caused by abnormal spatial relationships among the teeth, jaws, and facial structures[1], and fixed orthodontic treatment remains one of the primary therapeutic approaches for such conditions. During the course of treatment, positional deviations of individual teeth may occur in the fine-tuning phase due to bracket structure design and bonding inaccuracies. However, rebonding the brackets can compromise their structural integrity and significantly prolong treatment duration[2,3,4]. To address this, clinicians commonly bend stainless steel archwires into specific configurations that generate orthodontic forces in desired directions to reposition the teeth accurately. The intrusion arch is one of the most widely used archwire configurations in clinical practice. It delivers intrusive orthodontic force, which, if excessive, may lead to tooth mobility, root resorption, and alveolar bone loss[5,6], with the maxillary and mandibular anterior teeth being particularly susceptible[7].Currently, there exists no established method to predict the orthodontic force generated by an intrusion arch. In most cases, clinicians rely solely on their empirical experience to guide its application. Therefore, elucidating the quantitative relationship between the design parameters of the intrusion arch and the resulting orthodontic force is essential for enabling its parameterized representation and providing a theoretical basis for the rational application of force in clinical settings.

In addition, to visualize orthodontic force values, researchers have employed various approaches, including in vitro measurements, theoretical modeling, and finite element analysis. In 2021, Fumi et al.[8]conducted dynamic measurements of orthodontic force generated by archwires during tooth alignment using a custom-fabricated force-measuring apparatus. Their findings indicated a correlation between the magnitude of orthodontic force and the degree of dental crowding. Mayer et al.[9]constructed an in vitro measurement platform to quantify the range of orthodontic forces released by various nickel-titanium wires under specific tooth alignment conditions. However, the generalizability of their results was limited due to the experimental setup configurations. Zamani et al.[10]employed thin-film pressure sensors combined with image processing techniques to visualize both the magnitude and distribution of orthodontic force. Jiang[11], Ahmad[12], and Ma[13] independently utilized theoretical modeling and finite element models to predict orthodontic forces, reporting prediction errors of 3.24%, 9.55%, and 3.61%, respectively. Although these studies successfully captured the variation trends of orthodontic force during treatment and demonstrated the high predictive capability of finite element simulation, orthodontists are still unable to directly derive accurate force values from clinically available measurement data. As a result, the precise prediction of orthodontic force in clinical practice remains a significant challenge.

Multiple regression analysis (MRA) and artificial neural networks (ANN) are widely used tools for modeling linear and nonlinear relationships among variables, and have demonstrated broad applicability in force prediction tasks[14,15,16] . Accordingly, this study leverages a large dataset of experimental measurements to explore the quantitative relationship between orthodontic force and the structural parameters of the intrusion arch, utilizing both MRA and ANN. Despite the potential significance of this approach, no relevant studies have been identified to date.

The primary objectives of this study are: first, to identify the structural factors influencing the orthodontic force generated by the intrusion arch based on beam bending deformation theory; second, to construct an orthodontic force measurement platform and establish a comprehensive database; and third, to analyze the correlation between various structural features of the intrusion arch and the resulting orthodontic force, thereby providing a theoretical foundation for clinical modulation of force application. Furthermore, this study aims to establish an MRA-based orthodontic force prediction model to achieve parameterized expression of the relationships between structural factors and orthodontic force, as well as to construct an ANN-based prediction model and compare its performance with the MRA model in order to determine the optimal predictive method.

PROTOCOL:

Factors influencing the orthodontic force of the intrusion arch

When a preload is applied to the intrusion arch, both the horizontal arm and the anchorage arm of the arch exhibit varying degrees of deflection, as illustrated in Figure 1. Based on the theory of beam bending deformation and the principle of force composition, the deflection of these two components is calculated separately to establish a comprehensive prediction model for the orthodontic force generated by the intrusion arch. Moreover, since the maxillary anterior teeth are most closely related to patients' aesthetic appearance17 and are most susceptible to root resorption18,19, this study selects the intrusion arch of the left maxillary central incisor as the object of investigation.

The key variables used in the mechanical analysis of the intrusion arch are defined as follows and are referenced in both the equations and **Figure 1**:

θ: bending angle of the arch

d: length of the anchorage arm

lh: vertical displacement of the horizontal arm

la: vertical displacement of the anchorage arm

These parameters are incorporated into the bending deformation model described in Equations (1–5), based on the beam theory.

Furthermore, the intrusion arch is structurally symmetrical on both sides, so it suffices to analyze only one half of the symmetrical structure. According to the beam bending deformation theory, analysis of the anchorage arm of the intrusion arch yields the following approximate differential equation for its deflection curve：

$$\frac{d^2v(x_a)}{dx_a^2}=\frac{M(x_a)}{\mathrm{EI}_z} \quad \textbf{(1)}$$

By performing multiple integrations of Equation (1) and substituting the appropriate boundary conditions, and then ultimately applying the principle of force interaction, the orthodontic component force Fa is derived as the reaction force to the force Pa required to generate deformation in the anchorage arm of the intrusion arch. The orthodontic force generated by the bilateral anchorage arms is given by:

$$F_a=-P_a=\frac{6l_aEI_z}{d^3} \quad \textbf{(2)}$$

Where Iz is the moment of inertia of the cross-section of the archwire in the anchorage arm, and E is the elastic modulus of the archwire material.

In addition, the deformation behavior of the horizontal arm of the intrusion arch is analogous to that of the anchorage arm. Therefore, using the same mechanical modeling approach, the orthodontic force generated by the horizontal arm can be expressed as:

$$F_{\mathrm{h}}=-P_{\mathrm{h}}=\frac{48l_{\mathrm{h}}EI_z}{m^3} \quad \textbf{(3)}$$

Furthermore, from the loading analysis of the intrusion arch, the following relationship is derived:

$$l_h + l_a = h \qquad \textbf{(4)}$$

According to the principle of force composition, the orthodontic force generated by the intrusion arch is the resultant force F, arising from the restoring forces of the deformed anchorage arm and horizontal arm:

$$F = F_a + F_h = \frac{6 l_a E I_z}{d^3} + \frac{48 l_h E I_z}{m^3} \qquad \textbf{(5)}$$

To facilitate experimental investigation, the anchorage distance of the intrusion arch was fixed at 16 mm, based on the measurements of maxillary anterior crown widths reported by M20 and colleagues. Aside from this, under the condition of selecting a specific arch wire material with known properties, the orthodontic force can be modulated by adjusting the bending angle of the intrusion arch. However, this factor was not incorporated into the theoretical modeling. Moreover, with the anchorage distance held constant, the anchorage arm length and the arch length (i.e., horizontal arm length) exhibit a high degree of collinearity in subsequent analyses. Therefore, in this study, only the arch length, arch height, and bending angle were selected as independent variables, while the orthodontic force generated by the intrusion arch was designated as the dependent variable.

Establishment of the database

This study primarily investigates the quantitative relationship between the length, height, and bending angle of the intrusion arch and the resulting orthodontic force. A randomized combination of these characteristic parameters was employed to generate samples, and both the corresponding orthodontic force and structural parameters were measured. Rectangular stainless steel archwires with dimensions of 0.016 × 0.022 inches were used. A total of 300 intrusion arch samples were fabricated—250 for the training set and 50 for the testing set—by multiple clinicians following standardized bending procedures. The intrusion arch was fabricated using 0.016 × 0.022-inch stainless steel archwire with a standardized bending jig set to maintain consistent angles. Bending force was manually applied by calibrated orthodontic pliers, ensuring deviations in height and bilateral angle remained within 0.2 mm and 1°, respectively, across all 300 samples.

The dataset was randomly divided into a training set (250 samples) and a testing set (50 samples) using simple random sampling without stratification. This method aimed to maintain a consistent distribution of key structural parameters (arch length, height, and bending angle) across both sets. Although only a single random split was employed in this study, the relatively large training-to-testing ratio (5:1) and the consistent performance metrics observed across both sets support the model's generalizability.

Three experienced orthodontists independently measured the structural parameters of the intrusion arches. Samples were screened based on the following inclusion criteria: vertical height difference between bilateral intrusion arms less than 0.2 mm, and bilateral bending angle deviation less than 1°. Ultimately, 300 valid experimental samples were included. The mean value of each parameter was recorded to represent its corresponding measurement.

An in vitro measurement platform was constructed to simulate the clinical placement of the intrusion arch, as illustrated in Figure 2. The measuring apparatus consisted of an upper machine, signal transmitter, communication conversion module, pressure sensor, compression module, and micrometer fine-adjustment knob. The platform was composed of a micro motion stage, orthodontic brackets, simulation of the teeth, an anchorage distance locator ruler and pointer, a connecting frame, and other structural components.

The pressure sensor used in the experiment had a measurement range of 0–100 N and a resolution of 0.01 N. In the experimental setup, copper posts on the left and right sides were used to simulate the right maxillary central incisor and the left maxillary lateral incisor as bilateral anchorage teeth. Brackets were bonded at equal height positions on both copper posts, ensuring that the bracket height exceeded the maximum height of any intrusion arch sample. According to the experimental requirements, the distance between the bilateral copper posts was adjusted and fixed at 16 mm to simulate the horizontal distance between the two anchorage teeth in the oral cavity. The midpoint of the horizontal line connecting the two brackets was defined as the virtual location of the target tooth bracket, which also served as the horizontal target position for the downward movement of the compression module.

During the measurement of orthodontic force produced by the intrusion arch, to concretize the horizontal target position, the scale on the micrometer was recorded and marked when the compression module descended to the target position. For each sample measurement, the intrusion arch was mounted between the two brackets, ensuring the midpoint of the arch was aligned with the compression module. The micrometer was adjusted to the previously marked scale to ensure that the compression module reached the same horizontal target position each time. The orthodontic force was then recorded at this position. As the archwire undergoes varying degrees of plastic deformation after the first measurement, each sample was measured only once to minimize error. The measurement results were compiled into a database and analyzed separately for the training and testing sets. The results are shown in **Table 1**.

Construction of the predictive model for orthodontic force generated by intrusion arch multiple regression analysis (MRA), as a mathematical and statistical technique, can be broadly categorized into linear and nonlinear regression models based on the functional relationship between independent and dependent variables. Among them, the multiple linear regression analysis (MLA) model is generally expressed as follows:

$$y = \beta_0 + \beta_1 X_1 + \beta_2 X_2 + \ldots \beta_p X_p + \varepsilon \qquad \textbf{(6)}$$

Where y denotes the dependent variable; X_1, X_2 , …,X_p represent the independent variables; β_0 is the constant term (intercept); β_1, β_2, and β_p are the regression coefficients; ε is the random error term; and p > 1.

The MNLA model allows for various functional forms to describe the relationships among variables, and parameter estimation requires the use of optimization algorithms. In this study, the least squares method is employed to determine the optimal regression parameters. In addition, a predictive model for orthodontic force based on ANN is proposed.

An artificial neural network (ANN) is a machine learning technique inspired by biological neuronal systems21. In this research, we propose the use of a backpropagation artificial neural network (BP-ANN), an ANN architecture with an input layer, hidden layer(s), and output layer (as shown in Figure 3). The input features used in our predictions—arch height, arch length, and bending angle—can all be easily determined by clinicians, as they are part of standard clinical procedures. Furthermore, since orthodontic force can arise from the coupling of various factors, the proposed ANN with three hidden layers will more accurately describe the mapping relationship between the three input features and orthodontic force. The selection of the ANN architecture, with three hidden layers with six neurons in each, was based on a trial-and-error approach. We tested several configurations by varying the number of hidden layers (from 1 to 4) and the number of neurons per layer (from 3 to 10). The chosen structure yielded the lowest validation loss and highest predictive accuracy without signs of overfitting.

The ANN employs the ReLU function and the Sigmoid function as nonlinear activation functions, expressed as follows:

$$f(x)=\frac{1}{1+e^{-x}} \quad \textbf{(7)}$$

$$f(x)=max(0,x) \quad \textbf{(8)}$$

In this study, the mean squared error (MSE) is adopted as the loss function, along with the Adam optimization algorithm. The gradient of the MSE loss decreases as the training error reduces and is defined as:

$$MSE=\frac{\sum_{i=1}^{n}(x-y)^2}{n} \quad \textbf{(9)}$$

where x denotes the predicted value, y represents the measured value from the training samples, and n is the number of samples.

To ensure that the MSE decreases steadily and converges efficiently, the Adam optimizer is integrated into the ANN architecture. By combining momentum and adaptive learning rates, the model parameters are iteratively updated to improve training efficiency.

Finally, the performance of the predictive models is evaluated using RMSE, MAE, MAPE, and coefficient of determination (R^2), defined as follows:

$$\text{RMSE}=\sqrt{\frac{\sum_{i=1}^{n}(y-x)^2}{n}} \quad \textbf{(10)}$$

$$\text{MAE}=\frac{1}{n}\sum_{i=1}^{n}|y-x| \quad \textbf{(11)}$$

$$\text{MAPE}=\left(\frac{1}{n}\sum_{i=1}^{n}\left|\frac{y-x}{y}\right|\right)\times 100\% \quad \textbf{(12)}$$

$$R_2=1-\left(\frac{\sum(y-x)^2}{\sum(y-\bar{y})^2}\right) \quad \textbf{(13)}$$

where $\bar{y}$ denotes the mean of the measured values.

Moreover, samples were ideally randomized into training and testing datasets to eliminate bias. While some small residual error existed, the subsequent RMSE, MAE, MAPE, and R^2 metrics were used to assess its impact, ensuring dependability and model robustness with respect to the predictive capability of the model.

The protocol presented in this study includes theoretical modeling, standardized sample preparation, in vitro force measurements, and predictive model development using MRA and ANN. This systematic approach provides a strong framework for evaluating the relationship between key structural parameters of an intrusion arch and the orthodontic force it generates.

RESULTS:

Correlation analysis between the orthodontic force generated by the intrusion arch and its structural parameters

Table 2 demonstrates the correlation between each structural parameter and the orthodontic force at the 0.01 level of significance. Among them, the height of the intrusion arch exhibits the strongest positive correlation with the orthodontic force, with a Pearson correlation coefficient of 0.886. In contrast, the bending angle shows a significant negative correlation with the orthodontic force, with a Pearson correlation coefficient of -0.454, indicating that an increase in the bending angle leads to a marked decrease in the generated orthodontic force.

**Correlation is significant at the 0.01 level (two-tailed).

MLA model results

In the Multiple Linear Analysis (MLA) model, orthodontic force is designated as the dependent variable (y), with height (x_1), length (x_2), and bending angle (x_3) included as independent variables in a linear regression. The MLA model was subjected to t-tests, F-test, and multicollinearity diagnostics. The results are presented in Table 3. The developed regression model is expressed in Equation (14):

$$y = 14.168 + 8.335x_1 - 0.348x_2 - 0.032x_3 \quad \mathbf{(14)}$$

As shown in Table 3, based on the t-values and significance tests, the height, length, and bending angle of the intrusion arch all have statistically significant effects on the orthodontic force. Moreover, the variance inflation factor (VIF) values for all structural parameters are less than 5, indicating a low degree of multicollinearity among the variables. The goodness-of-fit between the predicted and measured values for both the training and testing sets is illustrated in Figure 4, with R^2 values of 0.806 and 0.743, respectively.

Results of the MNLA model

The MNLA model employs various commonly used functional forms to determine the most suitable equation for predicting orthodontic force, under the condition of maximizing the coefficient of determination (R^2). Table 4 presents the functional forms considered and their corresponding adjusted R^2 values.As can be seen from Table 4, the quadratic function yields the highest goodness-of-fit, with an R^2 value of 0.937.Its expanded polynomial form is expressed as follows:

$$y = \beta_0 + \beta_1 X_1 + \beta_2 X_2 + \beta_3 X_3 + \beta_4 X_1^2 + \beta_5 X_2^2 + \beta_6 X_3^2$$

$$+ \beta_7 X_1 X_2 + \beta_8 X_1 X_3 + \beta_9 X_2 X_3 \quad \mathbf{(15)}$$

According to Table 5, the regression model shows high overall significance, with an F-statistic of 394.24, indicating a robust fit. Based on the results in Table 5, the optimal regression model is expressed as:

$$y = -36.36 + 32.93X_1 + 2.133X_2 + 0.302X_3 - 4.825X_1^2 - 0.071X_2^2$$

$$- 0.001X_3^2 - 0.53X_1X_2 - 0.028X_1X_3 - 0.004X_2X_3 \quad \mathbf{(16)}$$

The fit between predicted and measured values for both the training and testing sets using the MNLA model is illustrated in **Figure 5**. The high R^2 values (0.934 for the training set and 0.900 for the testing set) confirm the model's excellent predictive capability.

Prediction of orthodontic force generated by the intrusion arch using ANN

During network training, five samples were input per batch, and the network was trained over 500 epochs. The learning rate was set to 0.001. To prevent overfitting, the model was evaluated against the testing set at the end of each epoch, and the corresponding error loss was recorded. The loss curve for the training process is shown in **Figure 6**.

The prediction performance of the ANN models constructed using two different activation functions was evaluated by examining the goodness-of-fit between predicted and measured values in both the training and testing sets, as shown in **Figure 7** and **Figure 8**. In comparison, the ANN model utilizing the ReLU activation function demonstrated superior predictive performance, with R^2 values of 0.895 in the training set and 0.834 in the testing set, both higher than those of the Sigmoid-based model, which yielded R^2 values of 0.822 and 0.816, respectively, **as shown in Figure 9.**

Comparison of the predictive performance between MRA and ANN models for orthodontic force generated by the intrusion arch

The predictive performance of the four models was evaluated using RMSE, MAE, MAPE, and coefficient of determination (R^2), as presented in **Table 6**. Overall, the MNLA model demonstrated the best predictive performance for orthodontic force in both the training and testing datasets.

The comparative performance of the four predictive models is further visualized in **Figure 10** and **Figure 11**. **Figure 10** illustrates the agreement between predicted and measured orthodontic force values, where the MNLA model shows minimal deviation. **Figure 11** presents box plots of prediction errors, clearly highlighting the MNLA model's lower and more consistent errors across both training and testing sets, confirming its superior predictive performance.

FIGURE AND TABLE LEGENDS:

Figure 1: Deflection behavior of the intrusion arch before and after loading. (**A**) Maxillary arch showing the position of the intrusion arch. (**B**) Enlarged schematic view showing key parameters and after loading (dashed black line).

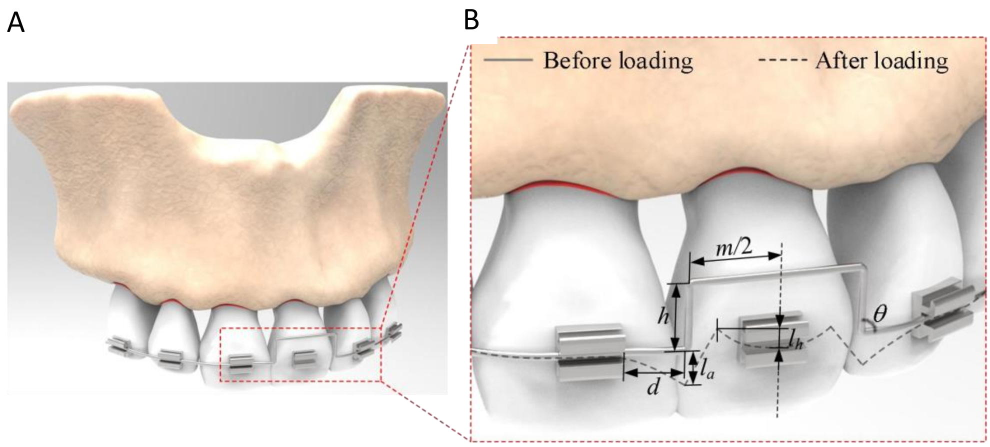

(A) Maxillary arch showing the position of the intrusion arch.
(B) Enlarged schematic view showing key parameters and after loading (dashed black line).m : length of the horizontal arm; h : height of the arch， θ: bending angle; d: length of the anchorage arm; lh : vertical displacement of the horizontal arm; la : vertical displacement of the anchorage arm.

Figure 2: *In vitro* experimental setup for measuring orthodontic force generated by the intrusion arch.

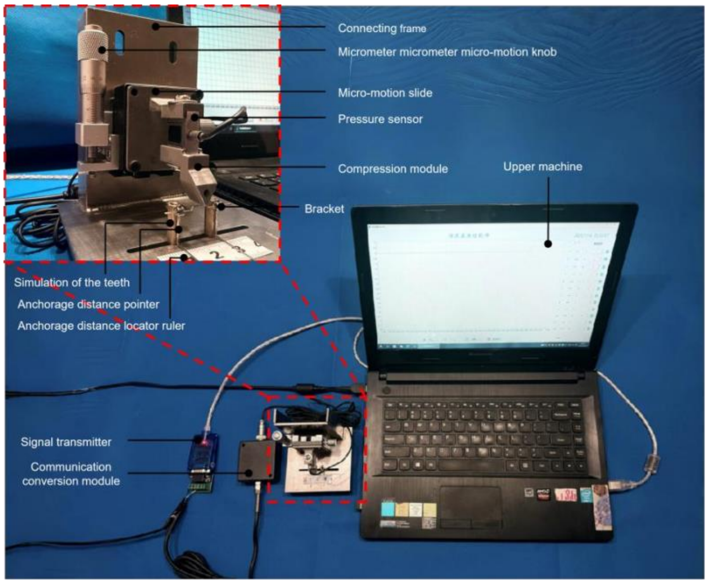

Figure 3: Architecture of the Artificial Neural Network model for predicting orthodontic force generated by the intrusion arch.

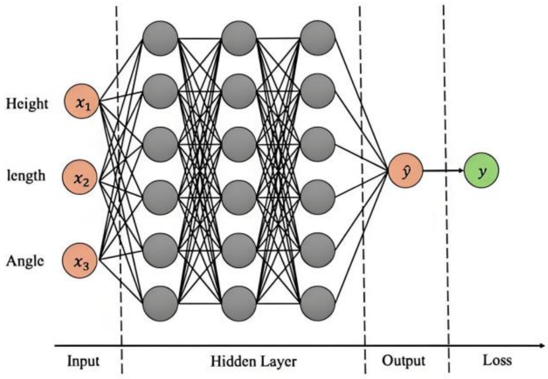

Figure 4: Goodness-of-fit between predicted and measured orthodontic force in the Multiple Linear Analysis model. (**A**) Training dataset; (**B**) Testing dataset.

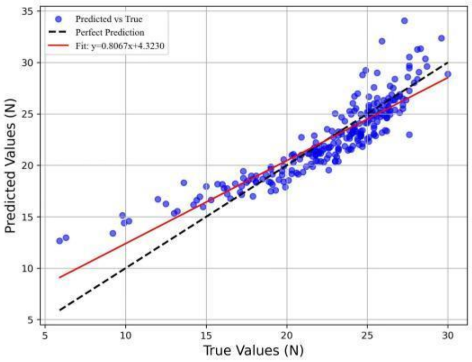

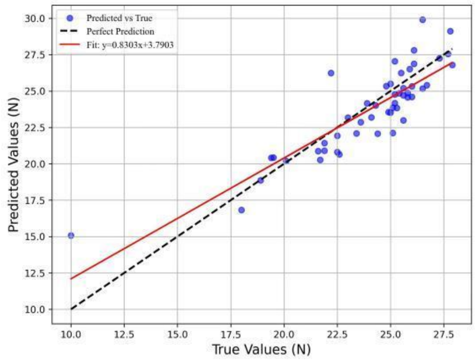

A) Training dataset	B) Testing dataset

Figure 5: Goodness-of-fit between predicted and measured orthodontic force in the Multiple Nonlinear Regression Analysis model. (**A**) Training dataset; (**B**) Testing dataset.

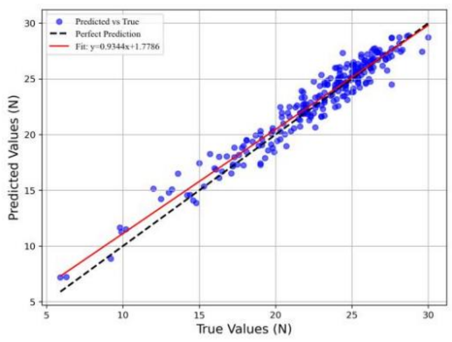

A) Training dataset

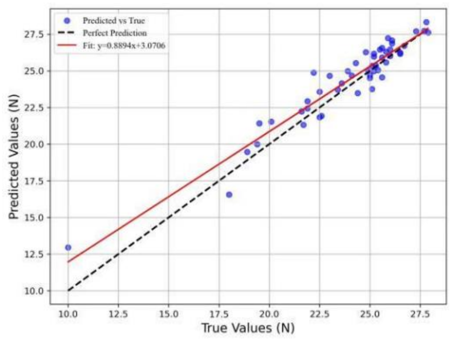

B) Testing dataset

Figure 6: Training loss curve of the Artificial Neural Network model during orthodontic force prediction.

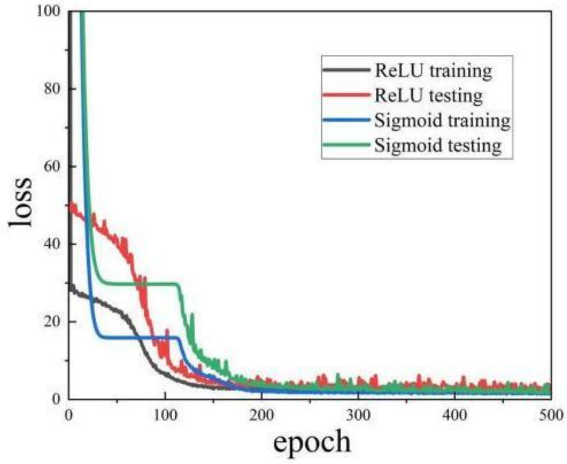

Figure 7: Fitting performance of the Artificial Neural Network model using the Rectified Linear Unit activation function. (**A**) Training dataset; (**B**) Testing dataset.

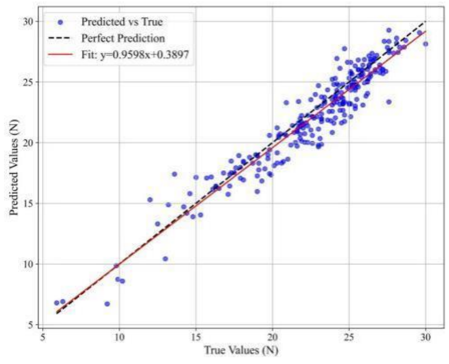

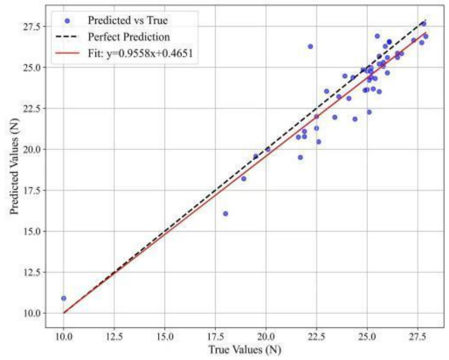

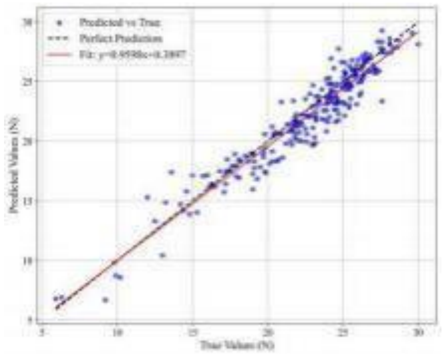

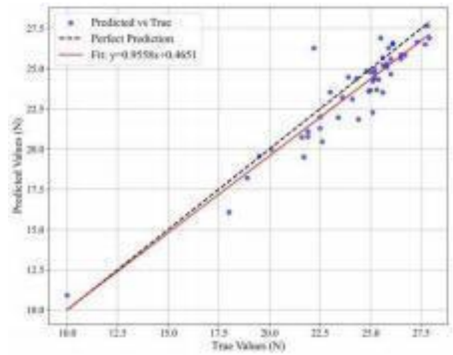

A) Training dataset	B) Testing dataset

Figure 8: Fitting performance of the Artificial Neural Network model using the Sigmoid activation function. (**A**) Training dataset; (**B**) Testing dataset.

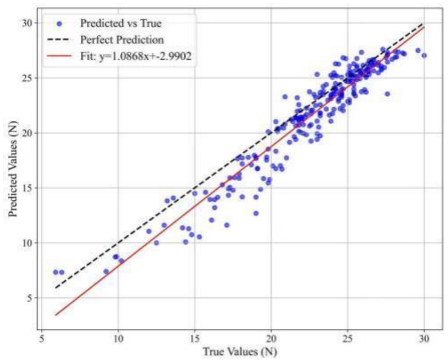	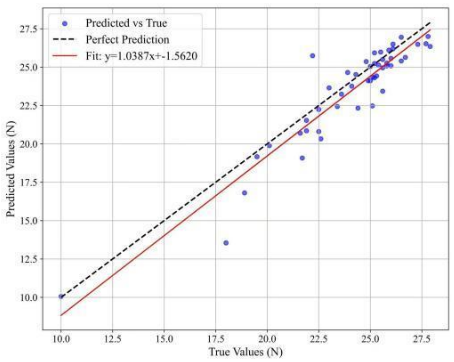
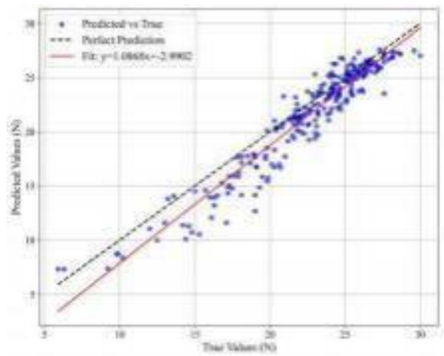	
A) Training dataset	B) Testing dataset

Figure 8. Fitting performance of the ANN (Sigmoid) model: a) training set; b) testing set

Figure 9: Activation functions used in the Artificial Neural Network models. (**A**) Rectified Linear Unit function; (**B**) Sigmoid function.

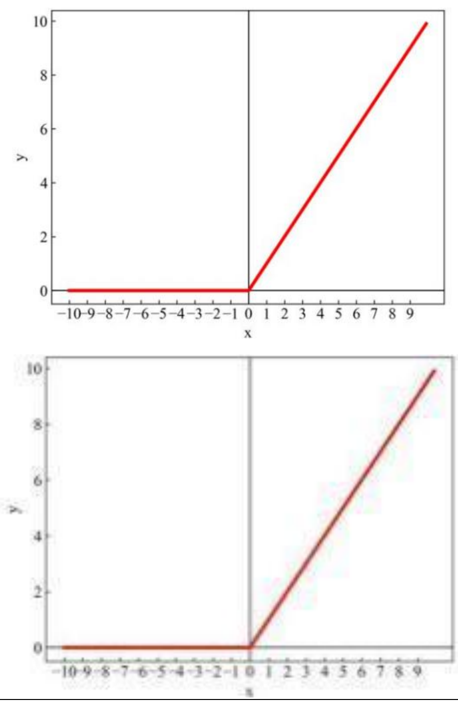

A) ReLU function

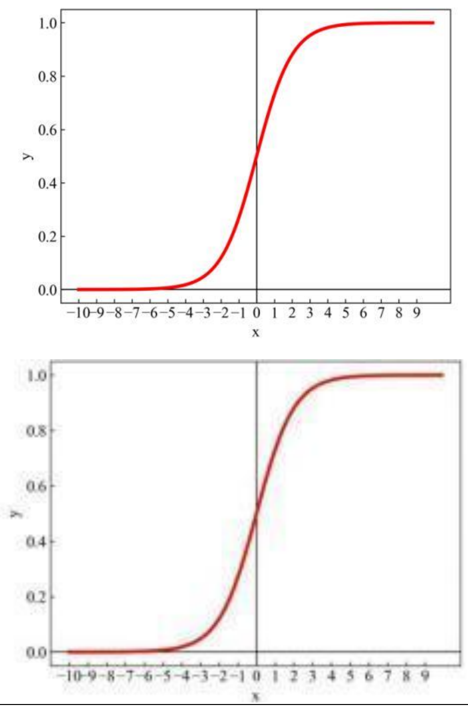

B) Sigmoid function

Figure 10: Comparison between measured and predicted orthodontic force values across all four predictive models—Multiple Linear Analysis, Multiple Nonlinear Regression Analysis, ANN (ReLU), and ANN (Sigmoid). (**A**) Training dataset; (**B**) Testing dataset. Abbreviations: ANN = Artificial Neural Network; MLA = Multiple Linear Analysis; MNLA = Multiple Nonlinear Regression Analysis; ReLU = Rectified Linear Unit.

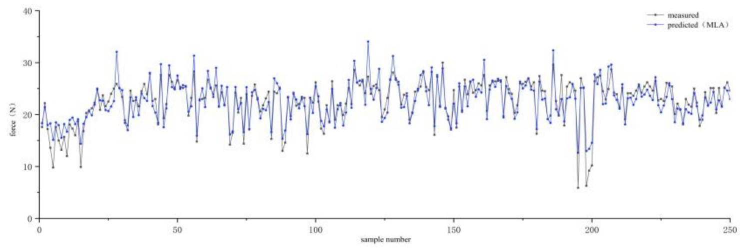

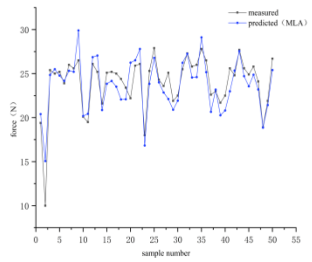

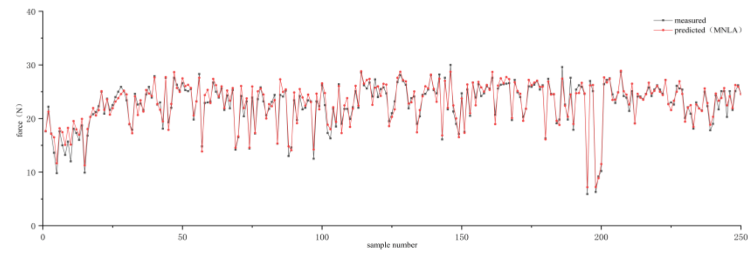

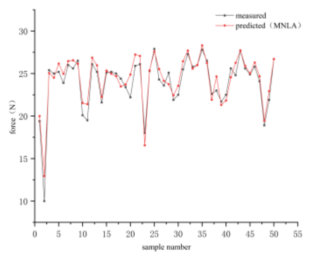

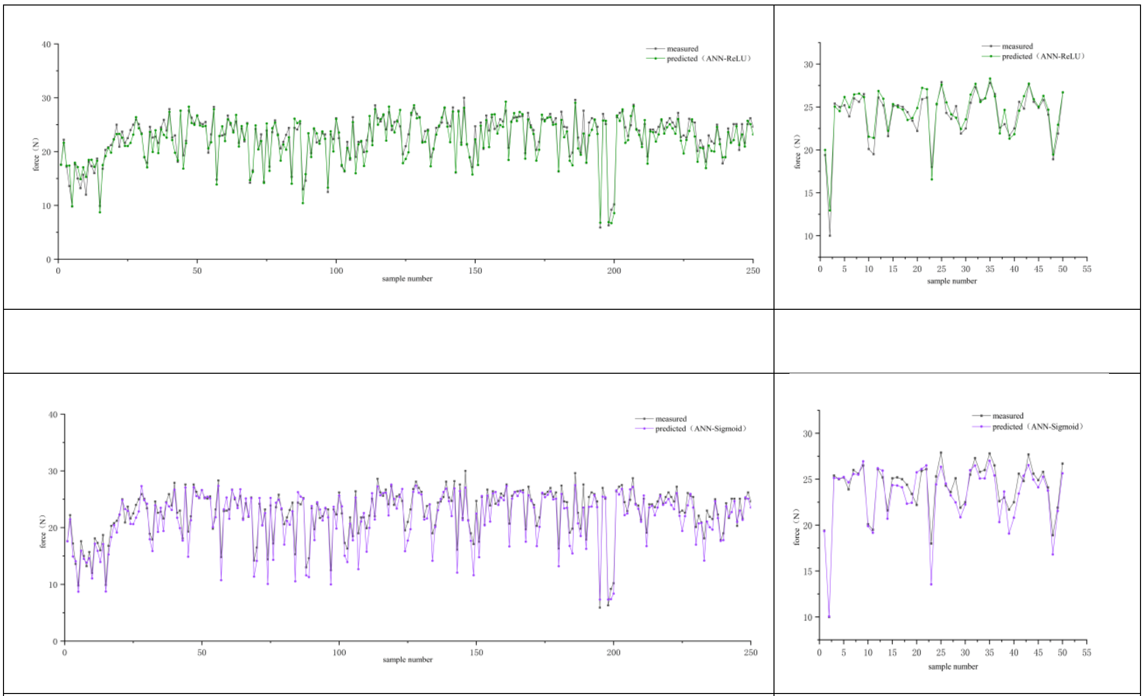

A） Training dataset

B） Testing dataset

Figure 11: Box plots of prediction errors for all four models—Multiple Linear Analysis, Multiple Nonlinear Regression Analysis, Artificial Neural Network with Rectified Linear Unit, and Artificial Neural Network with Sigmoid in the training and testing datasets. (**A**) Training dataset; (**B**) Testing dataset. Abbreviations: ANN = Artificial Neural Network; MLA = Multiple Linear Analysis; MNLA = Multiple Nonlinear Regression Analysis; ReLU = Rectified Linear Unit.

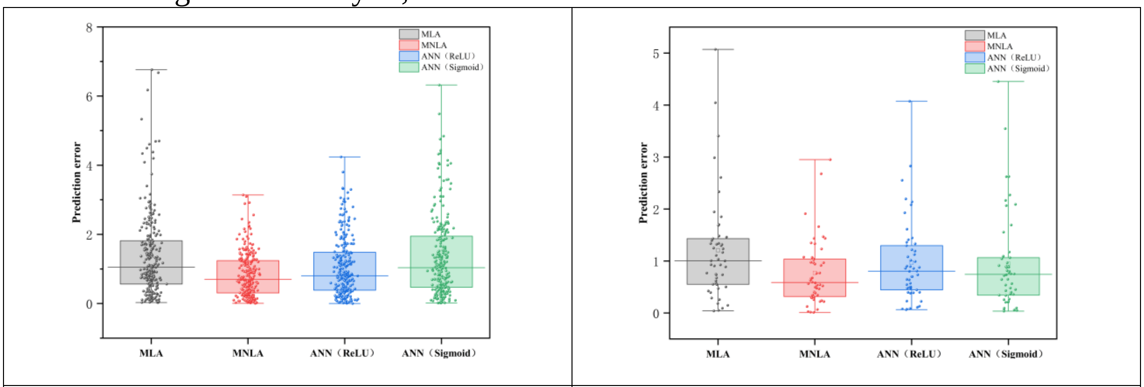

A) Training dataset

B) Testing dataset

Table 1: Descriptive statistics of structural parameters (height, length, and bending angle) and orthodontic force for intrusion arch samples used in training and testing sets.

Table 1-1. Descriptive statistics of characteristic parameters and orthodontic force for 250 training set samples

	Min	Max	Mean	Std,Dev
Height(mm)	0.61	3.16	1.77	0.45
Length(mm)	4.34	10.53	7.15	1.31
Angle(°)	90.00	155.00	121.53	11.97

Force(N)	5.90	30.00	22.81	4.14

Table 1-2. Descriptive statistics of characteristic parameters and orthodontic force for 50 testing set samples

	Min	Max	Mean	Std,Dev
Height(mm)	0.90	2.70	1.92	0.35
Length(mm)	5.25	10.18	7.18	0.49
Angle(°)	90.00	140.00	122.74	6.53
Force(N)	5.90	30.00	22.61	3.65

Table 2: Correlation analysis between orthodontic force generated by the intrusion arch and key structural parameters (arch height, arch length, and bending angle).

	Height(mm)	Length(mm)	Angle (°)	Forth(N)
Height(mm)	1			
Length(mm)	.350**	1		
Angle (°)	-.401**	0.07	1	
Forth(N)	.886**	. 196**	-.454**	1

***Correlation is significant at the 0.01 level (2-tailed).*

Table 3: Statistical results of the Multiple Linear Analysis model, including regression coefficients and multicollinearity diagnostics.

Variable	*ß*	***t***	***p***	**TOL**	**VIF**
Constant	14.168	8.917	0.000	-	-
Height(mm)	8.335	26.407	0.000	0.696	1.437
Length(mm)	-0.348	-3.513	0.001	0.825	1.212
Angle (°)	-0.032	-2.860	0.005	0.789	1.267
R^2_{adj}	0.804		R^2	0.806	
F(*p*)	341.67		R	0.898	

Table 4: Comparison of commonly used nonlinear functional models with their corresponding adjusted coefficients of determination (R^2 values) for orthodontic force prediction.

Model	Function expression	Adjust R^2
Power function	y=axb+ε	0.804
Logarithmic function	y=a+bln(x)+ε	0.900
Quadratic function	y=a+bx+cx2+ε	0.937
Trigonometric function	y=a+bsinx+ε	0.780
Exponential function	y=a+bcx+ε	0.748

Variable	*β*	*t*	*p*	F
Constant	-36.360	-4.564	0.000	
X_1	32.930	11.250	0.000	
X_2	2.133	2.823	0.010	
X_3	0.302	3.010	0.000	
X_1^2	-4.825	-13.595	0.000	394.24
X_2^2	-0.071	-1.873	0.062	
X_3^2	-0.001	-2.795	0.006	
(X_1X_2)	-0.530	-3.684	0.000	
(X_1X_3)	-0.028	-1.540	0.125	
(X_2X_3)	-0.004	-0.949	0.344	

Table 5: Selection and evaluation of the optimal functional form for the Multiple Nonlinear Regression Analysis model based on statistical performance criteria.

Table 6: Evaluation metrics for all predictive models—Multiple Linear Analysis, Multiple Nonlinear Regression Analysis, Artificial Neural Network with Rectified Linear Unit, and ANN with Sigmoid activation—based on Root Mean Squared Error, Mean Absolute Error, Mean Absolute Percentage Error. Abbreviations: MLA = Multiple Linear Analysis; MNLA = Multiple Nonlinear Regression Analysis; ANN = Artificial Neural Network; ReLU = Rectified Linear Unit; RMSE = Root Mean Squared Error; MAE = Mean Absolute Error; MAPE = Mean Absolute Percentage Error.

	MLA		MNLA		ANN（ReLU）		ANN（Sigmoid）	
	training	testing	training	testing	training	testing	training	testing
RMSE	1.841	1.562	1.050	0.988	1.353	1.248	3.107	1.317
MAE	1.378	1.205	0.834	0.772	1.047	0.967	1.334	0.947
MAPE	7.34%	5.57%	4.09%	3.66%	4.96%	4. 17%	6.61%	4.09%
R^2	0.806	0.740	0.934	0.900	0.895	0.834	0.822	0.816

DISCUSSION:

The development and validation of predictive models for estimating orthodontic force generated by intrusion arches using Multiple Nonlinear Regression Analysis (MNLA) and Artificial Neural Networks (ANN) have been presented. By leveraging a comprehensive experimental dataset and integrating both statistical and machine learning methods, this work aims to offer clinicians a precise, data-driven tool for force estimation. The proposed models address a significant gap in clinical orthodontics, namely, the lack of reliable, real-time methods to predict orthodontic forces during the use of intrusion arches, thus moving beyond subjective estimations or resource-intensive simulations.

Various alternative approaches have been employed in previous studies to quantify orthodontic force. Finite element analysis (FEA), in vitro force sensors, and dynamic robotic simulations have been widely used. For instance, a robotic test setup simulating initial tooth movements revealed variability in force delivery among different NiTi archwires, with medium-force wires generating higher moments than light-force counterparts22. Similarly, degradation studies comparing elastomeric chains and NiTi coil springs demonstrated that the latter offers superior long-term stability in both oral and simulated environments23. Additionally, in vitro experiments on archwires of different materials and sizes confirmed that wire dimensions and overeruption levels significantly influence the generated force24. While such methods offer valuable biomechanical insights, they often involve complex setups, high cost, and limited clinical applicability. In contrast, the models proposed in this study provide a rapid, low-cost, and clinically adaptable alternative that can be easily incorporated into chairside decision-making tools.

The correlation analysis indicated a positive relationship between arch length and orthodontic force, with a Pearson correlation coefficient of 0.196. However, in the MLA model, the coefficient for arch length was -0.348. This discrepancy arises because the correlation derived from univariate analysis reflects the influence of arch length on orthodontic force without considering the interaction effects of other structural parameters. In contrast, the orthodontic force prediction model established by MNLA takes into account the combined effects of all characteristic parameters, thereby offering a more accurate and integrated representation of how these parameters influence orthodontic force.

A comparison of the training loss curves of the two ANN models using ReLU and Sigmoid as activation functions indicates that the model employing the ReLU activation function exhibits stable loss reduction and faster convergence. In contrast, the model using the Sigmoid activation function shows a period of slow loss decrease between batch 30 and batch 120, reflecting difficulty in convergence. This phenomenon may be attributed to the mathematical characteristics of the activation functions. As shown in Figure 9, the Sigmoid function nonlinearly maps input values to a range between 0 and 1; however, when the input values become excessively large or small, the gradients approach zero, or even vanish, making the network difficult to train and slowing convergence. Conversely, the ReLU function maintains a constant gradient of 1 when the input is greater than 0, thereby avoiding the vanishing gradient problem and facilitating faster model convergence.

The comparison between predicted and measured orthodontic force values in the training and testing sets is illustrated in Figure 10. The MNLA-based prediction model yielded orthodontic force values with minimal deviation from the measured values. Additionally, as shown in the box plots of prediction errors for the four models in Figure

11, the MNLA model exhibited overall lower and more centralized prediction errors compared to the other three models, indicating its superior stability and predictive performance. Based on the evaluation indicators RMSE, MAE, MAPE, and R^2, the MNLA prediction model demonstrated optimal performance. The RMSE values in the training and testing groups were 1.050 and 0.988, respectively; the MAE values were 0.834 and 0.772; and the MAPE values were 4.09% and 4.96%, respectively. All four indicators confirm the MNLA model's superior predictive accuracy. Secondly, both ANN models employing ReLU and Sigmoid activation functions as nonlinear mapping mechanisms for orthodontic force prediction demonstrated better predictive performance than the MLA model. This advantage can be attributed to the strength of ANNs in handling complex nonlinear relationships and capturing latent patterns within data.

Additionally, ANN models possess strong generalization capabilities, enabling them to better manage outliers and previously unseen samples. The predictive performance of the ANN (ReLU) model was comparable to that of the MNLA model, with MAPE values of 4.96% and 4. 17% in the training and testing sets, respectively. In contrast, the ANN (Sigmoid) model performed slightly worse than its ReLU counterpart, indicating that the ReLU activation function more effectively captures the nonlinear relationships between the characteristic parameters of the intrusion arch and the resulting orthodontic force. The MLA model exhibited relatively poor predictive capability, with MAPE values in the training and testing sets exceeding those of the MNLA model by 79.5% and 52.2%, respectively — reaching 7.34% and 5.57%. This further underscores that the orthodontic force generated by an intrusion arch is a complex, multivariate nonlinear problem influenced by multiple variables. Purely linear analyses, such as those employed in MLA, are therefore limited in their ability to accurately predict orthodontic force.

The proposed predictive models significantly advance orthodontics and biomechanical modeling by enabling precise, data-driven estimation of orthodontic force from intrusion arch geometry. This reduces reliance on empirical judgment and costly simulations, enhances treatment safety, and supports individualized force application. The MNLA model, in particular, provides clinicians with a robust tool for real-time clinical decision-making. The MNLA and ANN models can be applied in clinical orthodontics to predict optimal intrusion forces based on arch geometry, aiding personalized treatment planning and minimizing root resorption risks. In research, they support simulation studies and material testing by replacing time-consuming in vitro setups with predictive modeling, thereby streamlining experimental design and enhancing biomechanical insight. While univariate correlation analysis identified a weak positive association between arch length and orthodontic force ($r = 0.196$), the multivariate regression coefficient was negative. This apparent contradiction arises from nonlinear interaction effects among variables.

The MNLA model includes terms such as X1X2, X1X3, and X2X3, which account for the combined influence of arch height, length, and bending angle. These interactions significantly alter the marginal effect of each parameter when considered jointly, justifying the observed sign reversal and highlighting the necessity of multivariate modeling to capture complex biomechanical behavior accurately. From a clinical perspective, our model findings offer practical guidance. For instance, increasing the bending angle of the intrusion arch from 120° to 135° can reduce the generated orthodontic force by approximately 50%. In practical terms, the force generated without such adjustments can be several times greater than what is considered clinically safe, posing a significant risk of root damage if not carefully controlled. Given the strong negative correlation between bending angle and orthodontic force, this adjustment provides a non-invasive and easily implementable method to fine-tune applied force and reduce root resorption risk without necessitating archwire replacement. Such actionable insights enhance the clinical utility of the model and support safer, patient-specific orthodontic interventions.

The models were trained using rectangular stainless steel wires of a fixed dimension (0.016 × 0.022 inches); thus, generalizability to other materials or dimensions is limited. All measurements were conducted in vitro under controlled conditions, which may not fully replicate intraoral variables such as temperature, saliva, and biological tissue response. While the sample size (n = 300) was adequate for initial model development, further external validation using diverse clinical datasets is needed to ensure broad applicability. Future research should focus on integrating patient-specific anatomical data and expanding the model to accommodate a wider range of wire types and configurations.

CONCLUSION:

This study applied beam bending deformation theory to identify the structural parameters affecting the orthodontic force generated by intrusion arches, and compared four predictive models of orthodontic force established using both MRA and ANN. This study is among the first to compare the predictive capabilities of MNLA and ANN in orthodontic force modeling, offering a balanced approach that combines interpretability with nonlinear learning. Such integration enhances both theoretical insight and practical precision in clinical decision-making. The height of the intrusion arch was identified as the most influential factor affecting the orthodontic force generated by the intrusion arch, followed by the bending angle and the loop length. Among the three influencing factors, the bending angle exhibited a significant negative correlation with orthodontic force, suggesting that clinicians can reduce the force exerted by the intrusion arch—and thereby minimize root resorption—by increasing the bending angle. However, the influence of loop length on orthodontic force remains inconclusive and requires further investigation.

Among the four predictive models of orthodontic force developed using MRA and ANN, the Multiple Nonlinear Regression Analysis (MNLA) model demonstrated the best predictive performance, with MAPE values of 4.09% and 3.66%, indicating lower prediction error than those reported in previous studies. The next best-performing model was the ANN model employing the ReLU activation function. Additionally, MRA enabled the parametric expression of orthodontic force generated by the intrusion arch, thereby providing a theoretical foundation for the rational clinical application of such forces. Nevertheless, the intrusive force generated by the intrusion arch in this study substantially exceeded the threshold for safe orthodontic force. It is therefore recommended that the clinical use of intrusion arches be minimized to reduce the risk of root resorption caused by excessive intrusive forces. Although the ANN model with ReLU activation exhibited strong predictive performance, a modest performance gap between training and testing sets (R^2 = 0.895 vs. 0.834) suggests potential mild overfitting.

REFERENCES:

1.Arwa G ,Shadi G ,M P C , et al.Malocclusion and oral health-related quality of life among young Danish adults. Is there a difference between subjects who received orthodontic treatment during adolescence and subjects without treatment need? A cross-sectional study.[J].Acta odontologica Scandinavica.**80**(1),1-9(2021).
2.S R ,A R ,L K , et al.Material testing of reconditioned orthodontic brackets.[J].Journal of orofacial orthopedics = Fortschritte der

Kieferorthopadie : Organ/official journal Deutsche Gesellschaft fur Kieferorthopadie.73(6),454-66(2012).
3.Alexandru V ,Silviu E B ,Mariana P , et al.Effects of Composite Resin on the Enamel after Debonding: An In Vitro Study — Metal Brackets vs. Ceramic Brackets[J].Applied Sciences. 11(16),7353-7353(2021).
4.CakirE,Duman AN, Yildirim AZ,et al.Shear bond strength between orthodontic brackets and monolithic 4YTZP:Aninvitrostudy [J].Materials (Basel).16 (14),5173(2023).
5.Rodrigues M A D ,Butzke S A M ,Freire M T F , et al.A comparative study of the effect of the intrusion arch and straight wire mechanics on incisor root resorption: A randomized, controlled trial.[J].The Angle orthodontist.88(1),20-26(2018).
6. Miriam S ,Jawad A ,David K , et al.The consequences of orthodontic extrusion on previously intruded permanent incisors-A retrospective study.[J].Dental traumatology : official publication of International Association for Dental Traumatology.40(1),54-60(2023).
7.Artak H ,Anna A ,Isaqali M K , et al.Tooth root resorption: A review. [J].Science progress. 105(3),368504221109217-368504221109217(2022).
8.Fumi T ,Yu K ,Shugo H , et al.Development of a new evaluation method for orthodontic forces generated in individual patients.[J].Dental materials journal.40(6),1437-1444(2021).
9.Mayer T J ,Lapatki G B ,Schmidt F .Novel approach for characterizing clinical load application of superelastic orthodontic wires.[J].Dental materials : official publication of the Academy of Dental Materials.40(9),1487-1496(2024).
10.N. S. M. Zamani et al.Distributed Force Measurement and Mapping Using Pressure-Sensitive Film and Image Processing for Active and Passive Aligners on Orthodontic Attachments[J]. in IEEE Access. 10,52853-52865(2022).
11.Jn-Gang J ,Yi-Hao C ,Lei W , et al.Modeling and Experimentation of the Unidirectional Orthodontic Force of Second Sequential Loop Orthodontic Archwire.[J].Applied bionics and biomechanics.20205786593(2020).
12.Ahmad W ,Liang K ,Xiong J , et al.Precision Orthodontic Force Simulation Using Nodal Displacement-Based Archwire Loading Approach.[J].International journal for numerical methods in biomedical engineering.40(12),e3889(2024).
13.Jingang J ,Xuefeng M ,Yingshuai H , et al.Experimentation and Simulation of Second Sequential Loop Orthodontic Moment Prediction Modeling[J].IEEE Access.656258-56268(2018).
14.Younghwan K ,Hongseob O .Comparison between Multiple Regression Analysis, Polynomial Regression Analysis, and an Artificial Neural Network for Tensile Strength Prediction of BFRP and GFRP[J].Materials.14(17),4861-4861(2021).

15.Park S ,Choi M ,Kim D , et al.Modeling Yield Strength of Austenitic Stainless Steel Welds Using Multiple Regression Analysis and Machine Learning[J].Metals. 13(9),1625-(2023).
16.Huohai Y ,Binghong X ,Xuanyu L , et al.Breakdown Pressure Prediction of Tight Sandstone Horizontal Wells Based on the Mechanism Model and Multiple Linear Regression Model[J].Energies.15(19),6944-6944(2022).
17.Hideki I ,Sangwook K ,Takahiro S , et al.Effects of vertical positions of anterior teeth on smile esthetics in Japanese and korean orthodontists and orthodontic patients.[J].Journal of esthetic and restorative dentistry : official publication of the American Academy of Esthetic Dentistry ... [et al.].25(4),274-82(2013).
18.Miriam S ,Jawad A ,David K , et al.The consequences of orthodontic extrusion on previously intruded permanent incisors-A retrospective study.[J].Dental traumatology : official publication of International Association for Dental Traumatology.40(1),54-60(2023).
19.Satu A ,Sakari J P .Apical root resorption after orthodontic treatment -- a retrospective study.[J].European journal of orthodontics.29(4),408-12(2007).
20.Melo M ,Ata-Ali F ,Huertas J , et al.Revisiting the Maxillary Teeth in 384 Subjects Reveals A Deviation From the Classical Aesthetic Dimensions[J].Scientific Reports.9(1),1-9(2019).
21.AGATONOVIC-KUSTRIN S, BERESFORD R. Basic concepts of artificial neural network (ANN) modeling and its application in pharmaceutical research[J]. Journal of Pharmaceutical and Biomedical Analysis. 22(5), 717-727(2000).
22.Dotzer, B. et al. Biomechanical simulation of forces and moments of initial orthodontic tooth movement in dependence on the used archwire system by ROSS (Robot Orthodontic Measurement & Simulation System). *J Mech Behav Biomed Mater*. 144, 105960 (2023).
23.Yang, L. et al. Force degradation of two orthodontic accessories analyzed in vivo and in vitro. *BMC Oral Health*. 23 (1), 1001 (2023).
24.Wang, D. et al. Quantification of orthodontic loads on teeth in the correction of canine overeruption using different archwire designs. *Am J Orthod Dentofacial Orthop*. 163 (1), e13–e21 (2023).